



*entropy*



Article

---

# Evanescent Electron Wave-Spin

---

Ju Gao and Fang Shen



<https://doi.org/10.3390/e26090789>

# Evanescent Electron Wave-Spin

Ju Gao \* and Fang Shen

Department of Electrical and Computer Engineering, University of Illinois, Urbana, IL 61801, USA

\* Correspondence: jugao@illinois.edu

**Abstract:** This study demonstrates the existence of an evanescent electron wave outside both finite and infinite quantum wells by solving the Dirac equation and ensuring the continuity of the spinor wavefunction at the boundaries. We show that this evanescent wave shares the spin characteristics of the wave confined within the well, as indicated by analytical expressions for the current density across all regions. Our findings suggest that the electron cannot be confined to a mathematical singularity and that quantum information, or quantum entropy, can leak through any quantum confinement. These results emphasize that the electron wave, fully characterized by Lorentz-invariant charge and current densities, should be considered the true and sole entity of the electron.

**Keywords:** electron spin; quantum computing; spintronics; quantum mechanics interpretation

**PACS:** 3.50; 32.80; 42.50

## 1. Electron Wave-Spin

Electron spin, a fundamental property of electrons, plays a crucial role in advancing fields such as quantum computing and spintronics [1–3]. Despite its significance, the nature and origin of electron spin have been debated since its discovery over a century ago [4,5]. One of the main challenges is reconciling the concept of the electron as a spinning particle with the principles of special relativity. Additionally, the true radius of the electron's corpuscular charge ball or disk remains undetermined and unmeasured. This uncertainty has led many to view electron spin as an abstract property rooted in mathematical formalism rather than as a tangible physical entity.

However, alternative interpretations have been proposed [6,7] that relate electron spin to the physical quantity of current density,  $\mathbf{j}$ . In these frameworks, spin emerges as a measurable wave property because current density can be derived as an observable from the wavefunctions of the Dirac equation. Recently, we demonstrated the existence of stable circulating current densities of an electron within quantum wells [8]. The electron spin value of  $\hbar/2$  is obtained by integrating the interaction term,  $\mathbf{j} \cdot \mathbf{A}$ , between the current density and an external vector potential over the spatial extent of the wavefunctions. This spin value is further influenced by the geometry of the quantum well and the quantum numbers of the states, highlighting the wave nature of the electron spin. We have suggested that this effect can be quantitatively verified through abnormal Zeeman splitting experiments. Moreover, this electron wave-spin exhibits geometric and topological features that are absent in the traditional spinning particle model but could also be experimentally observed [9]. In summary, we assert it is the electron wave that is physically spinning.

Importantly, the circulating current density and charge density,  $\rho$ , together form a Lorentz-invariant four-current,  $(\rho, \mathbf{j})$ . If the electron wave behaves in accordance with special relativity, then the electron as a discrete corpuscular entity with a well-defined radius cannot spin or exist. This perspective suggests that the electron wave itself is the fundamental reality of the electron. By interpreting the electron purely as a physical wave, without invoking wave-particle duality, we provide a framework to reconcile some of the most perplexing aspects of quantum mechanics. For instance, the phenomenon of



**Citation:** Gao, J.; Shen, F. Evanescent Electron Wave-Spin. *Entropy* **2024**, *26*, 789. <https://doi.org/10.3390/e26090789>

Academic Editor: Alessandro Sergi

Received: 30 June 2024

Revised: 28 August 2024

Accepted: 4 September 2024

Published: 14 September 2024



**Copyright:** © 2024 by the authors. Licensee MDPI, Basel, Switzerland. This article is an open access article distributed under the terms and conditions of the Creative Commons Attribution (CC BY) license (<https://creativecommons.org/licenses/by/4.0/>).

an electron appearing in multiple locations simultaneously is naturally explained by its wave nature, while the correlation between two entangled electrons over a distance can be understood as the overlapping of two physical waves.

This wave-based perspective also has significant implications for practical applications in quantum devices, such as quantum wires, which have been extensively studied using Schrödinger's equations [10,11]. Since a wave cannot be entirely confined within a device, it becomes intriguing to explore the properties of the electron wave in the vicinity of the device as part of the overall electron entity. In our previous work, we examined the electron wave-spin within an infinite quantum well, where the wavefunction outside the well is typically assumed to be zero [12]. However, in reality, all potentials are finite, resulting in a non-negligible wavefunction outside the well. Of particular interest is the situation where the electron's eigenenergy is below the quantum well potential, leading to an evanescent wave that does not propagate but remains near the quantum well. We aim to study the spin properties of this evanescent wave and its relationship to the confined wave within the quantum well. This could open up possibilities for probing spin properties externally, without collapsing the spin state within the well, analogous to evanescent wave sensing in optics [13–15].

This paper is structured as follows: in Section 2, we rigorously solve the Dirac equation for an electron in a quantum well and derive analytical expressions for the corresponding wavefunctions. In Section 3, we calculate the current densities both inside and outside the quantum well, demonstrating the existence of an evanescent wave even in the case of an infinite quantum well. In Section 4, we focus on the spin behavior of the evanescent wave and discuss the broader implications for quantum mechanics interpretations and technological applications.

## 2. Dirac Electron in a Finite Cylindrical Quantum Well

Here, we derive exact solutions of the Dirac equation in a finite cylindrical quantum well and obtain analytical expressions for the current density. The eigenenergy values will be solved numerically through the boundary condition equations.

The Dirac equation in the cylindrical coordinate is

$$\frac{1}{c} \frac{\partial}{\partial t} \psi(\mathbf{r}, t) = \left\{ -\boldsymbol{\alpha} \cdot \nabla - i \frac{mc^2}{\hbar c} \gamma^0 - i \frac{1}{\hbar c} U(\mathbf{r}) \right\} \psi(\mathbf{r}, t), \quad (1)$$

where  $(\rho, \phi, z)$  represent polar, azimuthal angle, and  $z$  coordinate, respectively. The operator

$$\boldsymbol{\alpha} \cdot \nabla = \alpha_\rho \frac{\partial}{\partial \rho} + \alpha_\phi \frac{1}{\rho} \frac{\partial}{\partial \phi} + \alpha_z \frac{\partial}{\partial z} \quad (2)$$

contains  $\alpha$ -matrix in cylindrical coordinate

$$\begin{aligned} \alpha_\rho &= \begin{pmatrix} 0 & 0 & 0 & e^{-i\phi} \\ 0 & 0 & e^{i\phi} & 0 \\ 0 & e^{-i\phi} & 0 & 0 \\ e^{i\phi} & 0 & 0 & 0 \end{pmatrix}; \\ \alpha_\phi &= \begin{pmatrix} 0 & 0 & 0 & -ie^{-i\phi} \\ 0 & 0 & ie^{i\phi} & 0 \\ 0 & -ie^{-i\phi} & 0 & 0 \\ ie^{i\phi} & 0 & 0 & 0 \end{pmatrix}; \\ \alpha_z &= \begin{pmatrix} 0 & 0 & 1 & 0 \\ 0 & 0 & 0 & -1 \\ 1 & 0 & 0 & 0 \\ 0 & -1 & 0 & 0 \end{pmatrix}, \end{aligned} \quad (3)$$

with the following properties:

$$\begin{aligned} \sigma_\rho^2 &= \sigma_\phi^2 = \sigma_z^2 = 1, \\ \sigma_\rho\sigma_\phi &= i\alpha_z, \\ \sigma_\rho\sigma_\phi + \sigma_\phi\sigma_\rho &= 0. \end{aligned} \tag{4}$$

We now let the potential

$$U(\mathbf{r}) = U(\rho) = \begin{cases} 0, & \rho < R \\ U, & \rho > R \end{cases} \tag{5}$$

represent a finite cylindrical quantum well of potential  $U$  and radius  $R$ . The wavefunction in the quantum well can be expressed by the separation of variables

$$\psi(\mathbf{r}, t) = e^{-i\mathcal{E}t/\hbar} e^{iP_z z/\hbar} \tilde{\psi}(\phi, \rho), \tag{6}$$

where the electron is not confined along the  $z$ -direction and behaves as a traveling wave. We further assume the wavelength of the traveling wave is much larger than the size of the quantum well; thus, for our discussion,  $P_z = 0$ . The eigenenergy,  $\mathcal{E}$ , is determined by the boundary conditions later.

Plugging Equation (6) into Equation (1), we obtain the equation

$$\left\{ -i\frac{\mathcal{E}}{\hbar c} + \alpha_\rho \frac{\partial}{\partial \rho} + \alpha_\phi \frac{1}{\rho} \frac{\partial}{\partial \phi} + i\frac{mc^2}{\hbar c} \gamma^0 + i\frac{1}{\hbar c} U(\rho) \right\} \tilde{\psi}(\phi, \rho) = 0. \tag{7}$$

$\tilde{\psi}(\phi, \rho)$  is a four-spinor that can be written as

$$\tilde{\psi}(\phi, \rho) = \begin{pmatrix} \mu_A(\phi, \rho) \\ \mu_B(\phi, \rho) \end{pmatrix}, \tag{8}$$

where  $\mu_A(\phi, \rho)$  and  $\mu_B(\phi, \rho)$  are two component spinor wavefunctions, known as the large and small components of the Dirac wavefunctions, that follow the equations

$$\begin{aligned} -i\frac{\mathcal{E} - U(\rho) - mc^2}{\hbar c} \mu_A(\phi, \rho) &= \\ \begin{pmatrix} 0 & e^{-i\phi} \frac{\partial}{\partial \rho} - ie^{-i\phi} \frac{1}{\rho} \frac{\partial}{\partial \phi} \\ e^{i\phi} \frac{\partial}{\partial \rho} + ie^{i\phi} \frac{1}{\rho} \frac{\partial}{\partial \phi} & 0 \end{pmatrix} \mu_B(\phi, \rho); \\ -i\frac{\mathcal{E} - U(\rho) + mc^2}{\hbar c} \mu_B(\phi, \rho) &= \\ \begin{pmatrix} 0 & e^{-i\phi} \frac{\partial}{\partial \rho} - ie^{-i\phi} \frac{1}{\rho} \frac{\partial}{\partial \phi} \\ e^{i\phi} \frac{\partial}{\partial \rho} + ie^{i\phi} \frac{1}{\rho} \frac{\partial}{\partial \phi} & 0 \end{pmatrix} \mu_A(\phi, \rho). \end{aligned} \tag{9}$$

The above equations are combined to give the equation for  $\mu_A(\phi, \rho)$ ,

$$\left( \frac{\partial^2}{\partial \rho^2} + \frac{1}{\rho} \frac{\partial}{\partial \rho} + \frac{1}{\rho^2} \frac{\partial^2}{\partial \phi^2} \right) \mu_A(\phi, \rho) = \begin{cases} -\zeta^2 \mu_A(\rho), & \rho < R; \\ \xi^2 \mu_A(\rho), & \rho > R, \end{cases} \tag{10}$$

where  $\zeta$  and  $\xi$  are wave numbers inside and outside the quantum well, respectively,

$$\begin{aligned} \zeta &= \sqrt{\frac{\mathcal{E}^2 - m^2c^4}{\hbar^2c^2}}, \\ \xi &= \sqrt{\frac{m^2c^4 - (\mathcal{E} - U)^2}{\hbar^2c^2}}, \end{aligned} \tag{11}$$

and are both real numbers, since the quantum well potential falls in the range of

$$\mathcal{E} - mc^2 < U < mc^2. \tag{12}$$

We now separate the variables of  $\mu_A(\phi, \rho)$  for the spin-up electron,

$$\mu_A(\phi, \rho) = e^{il\phi} \mu_A(\rho) \begin{pmatrix} 1 \\ 0 \end{pmatrix}, \tag{13}$$

where  $l$  is the azimuthal quantum number for the angular wavefunction  $e^{il\phi}$ .

The radial wavefunction  $\mu_A(\rho)$  follows the equation by plugging Equation (13) into Equation (10),

$$\left( \frac{\partial^2}{\partial \rho^2} + \frac{1}{\rho} \frac{\partial}{\partial \rho} - \frac{l^2}{\rho^2} \right) \mu_A(\rho) = \begin{cases} -\zeta^2 \mu_A(\rho), & \rho < R; \\ \xi^2 \mu_A(\rho), & \rho > R. \end{cases} \tag{14}$$

$\mu_A(\rho)$  can be readily solved from Equation (14), and  $\mu_B(\phi, \rho)$  can be subsequently obtained from Equation (9). Finally, the four-component spinor wavefunction  $\tilde{\psi}(\phi, \rho)$  in Equation (8) for the spin-up electron is obtained:

$$\tilde{\psi}(\phi, \rho) = \begin{cases} e^{il\phi} \begin{pmatrix} J_l(\zeta\rho) \\ 0 \\ 0 \\ ie^{i\phi} \frac{\hbar c}{\mathcal{E} + mc^2} \left\{ \frac{1}{2} \zeta [J_{l-1}(\zeta\rho) - J_{l+1}(\zeta\rho)] - \frac{1}{\rho} J_l(\zeta\rho) \right\} \end{pmatrix}, & \rho \leq R; \\ e^{il\phi} \begin{pmatrix} \kappa K_l(\xi\rho) \\ 0 \\ 0 \\ ie^{i\phi} \kappa \frac{\hbar c}{\mathcal{E} - U + mc^2} \left\{ \frac{1}{2} \xi [-K_{l-1}(\xi\rho) - K_{l+1}(\xi\rho)] - \frac{1}{\rho} K_l(\xi\rho) \right\} \end{pmatrix}, & \rho > R, \end{cases} \tag{15}$$

where  $J_l$  and  $K_l$  are the Bessel function and modified Bessel functions of order  $l$ , respectively. The constant  $\kappa$  measures the relative magnitude between the wavefunctions inside and outside the quantum well.

We now apply the boundary condition to ensure that all components of the spinor wavefunction are continuous at  $\rho = R$ :

$$\begin{aligned} \kappa K_l(\xi R) &= J_l(\zeta R) \\ \kappa \left\{ \frac{1}{2} \xi [-K_{l-1}(\xi R) - K_{l+1}(\xi R)] - \frac{1}{R} K_l(\xi R) \right\} &= \\ \frac{\mathcal{E} - U + mc^2}{\mathcal{E} + mc^2} \left\{ \frac{1}{2} \zeta [J_{l-1}(\zeta R) - J_{l+1}(\zeta R)] - \frac{1}{R} J_l(\zeta R) \right\}, \end{aligned} \tag{16}$$

from which the eigenenergies  $\mathcal{E}_{ln}$  and constant  $\kappa$  can be solved numerically. Here,  $l$  and  $n$  denote the azimuthal and radial quantum numbers, respectively. Numerical calculations can then be carried out to study the wave properties in all regions.

The boundary conditions described in Equation (16) ensure the continuity of both the charge and current densities of the electron wave, while in the Schrödinger framework,

only charge continuity is typically considered. The continuity of the spinor wavefunction, thus, preserves the Lorentz invariance of the electron throughout, except when interacting with a Lorentz-violating field, as previously studied in [16]. In that study, the eigenenergy levels—and consequently the spectra—of a Dirac electron in a cylindrical potential well were analyzed to investigate the effects of classical gravity within the quantum mechanical regime. However, the wave effects, including wave-spin, were not explored, as it was stated on the third page of that paper that “we are not concerned with any global properties of the wave function in this work”.

### 3. Evanescent Electron Wave

To simplify the discussion on the evanescent electron wave, we choose the lowest azimuthal quantum number  $l = 0$ , and the wavefunction becomes

$$\tilde{\psi}(\phi, \rho) = \begin{cases} \begin{pmatrix} J_0(\zeta\rho) \\ 0 \\ 0 \\ -ie^{i\phi} \frac{\hbar c}{\mathcal{E} + mc^2} \frac{1}{2} \zeta J_1(\zeta\rho) \end{pmatrix}, & \rho \leq R; \\ \begin{pmatrix} \kappa K_0(\xi\rho) \\ 0 \\ 0 \\ -i\kappa e^{i\phi} \frac{\hbar c}{\mathcal{E} - U + mc^2} \frac{1}{2} \xi K_1(\xi\rho) \end{pmatrix}, & \rho > R. \end{cases} \quad (17)$$

The boundary conditions become

$$\begin{aligned} \kappa K_0(\xi R) &= J_0(\zeta R) \\ \kappa \xi K_1(\xi R) &= \frac{\mathcal{E} - U + mc^2}{\mathcal{E} + mc^2} \zeta J_1(\zeta R), \end{aligned} \quad (18)$$

which are combined to give the eigenvalue equation

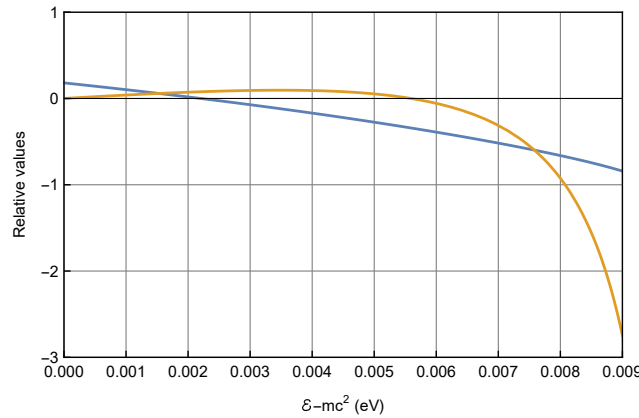
$$\xi J_0(\zeta R) K_1(\xi R) = \frac{\mathcal{E} - U + mc^2}{\mathcal{E} + mc^2} \zeta K_0(\xi R) J_1(\zeta R), \quad (19)$$

from which the eigenenergies  $\mathcal{E}$  and constant  $\kappa$  can be solved numerically.

We now conduct the numerical study by choosing a quantum well of radius  $R = 10$  nm and a series of potentials  $U = 0.01, 0.1, 1, 10$  eV. For each potential, multiple eigenenergies can be found by solving Equation (19) numerically. As an example, for  $U = 0.01$  eV, only two eigenenergies are found within the quantum well,  $\mathcal{E}_{01} - mc^2 = 1.53$  (meV) and  $\mathcal{E}_{02} - mc^2 = 7.63$  (meV), that correspond to the ground state and first excited state, respectively. Figure 1 shows the two eigenenergy solutions as the inception points of functions  $\xi J_0(\zeta R) K_1(\xi R)$  and  $\frac{\mathcal{E} - U + mc^2}{\mathcal{E} + mc^2} \zeta K_0(\xi R) J_1(\zeta R)$  from Equation (19).

We now calculate the ground state eigenenergies  $\mathcal{E}_{01} - mc^2$  and  $\kappa_{01}$  for all potentials, followed by the calculation of wave numbers  $\zeta_{01}$  and  $\xi_{01}$  with the help of Equation (11). The results are listed in Table 1.

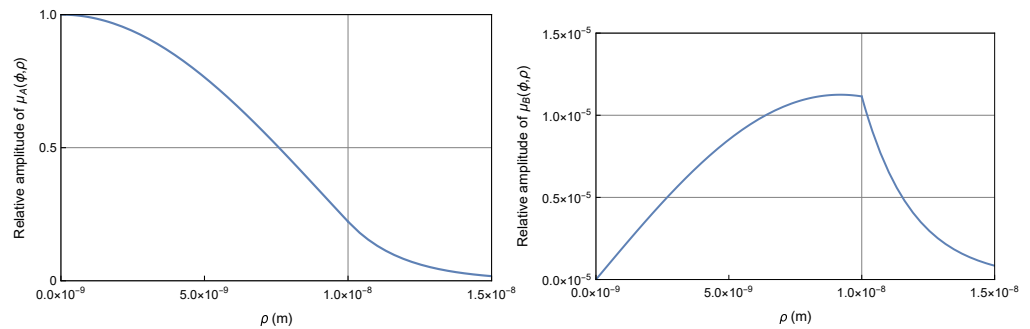
The numerical calculation shows that the electron wave tunnels out of the quantum well and behaves evanescently due to the characteristics of the modified Bessel functions. Figure 2 plots the wavefunctions inside and outside the well for the ground state of  $U = 0.01$  eV. It is shown that a substantial evanescent wave tunnels out of the quantum well, but satisfies wavefunction continuity at the boundary.



**Figure 1.** Numerical solution of the eigenenergies for the electron in a quantum well of  $U = 0.01$  eV and  $R = 10$  nm. The blue and orange curves representing  $\xi J_0(\xi R)K_1(\xi R)$  and  $\frac{\mathcal{E} - U + mc^2}{\mathcal{E} + mc^2} \zeta K_0(\zeta R)J_1(\zeta R)$  from Equation (19), respectively, intercept at eigenenergies  $\mathcal{E}_{01} - mc^2 = 1.53$ (meV) and  $7.63$ (meV) for the ground and excited state, respectively.

**Table 1.** Eigenenergy  $\mathcal{E}_{01}$  and relative constant  $\kappa_{01}$ .

$U$ (eV)	$\mathcal{E}_{01} - mc^2$ (meV)	$\kappa_{01}$	$\zeta_{01}(m^{-1})$	$\xi_{01}(m^{-1})$
0.01	1.53	44.1	$2.00 \times 10^8$	$4.71 \times 10^8$
0.10	1.95	$2.23 \times 10^6$	$2.26 \times 10^8$	$1.60 \times 10^9$
1.00	2.12	$2.32 \times 10^{21}$	$2.36 \times 10^8$	$5.12 \times 10^9$
10.0	2.18	$1.75 \times 10^{69}$	$2.39 \times 10^8$	$1.62 \times 10^{10}$



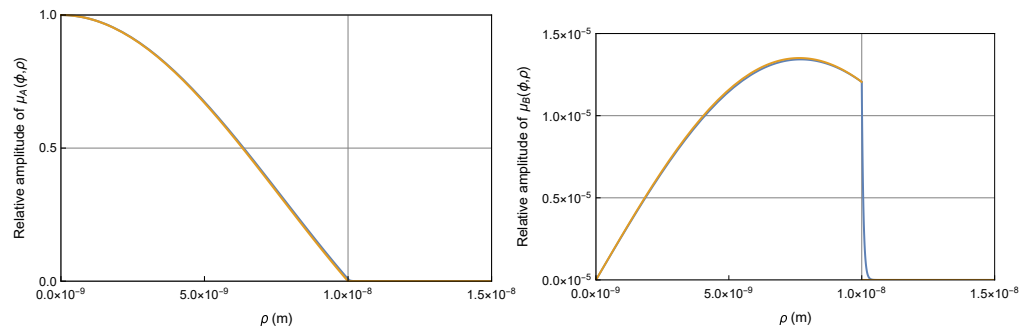
**Figure 2.** Wavefunction plots for the Dirac electron in a quantum well of  $U = 0.01$  eV and  $R = 10$  nm. The large component  $\mu_A(\phi, \rho)$  (left) and small component  $\mu_B(\phi, \rho)$  (right) wavefunctions demonstrate that a substantial evanescent wave tunnels out of the quantum well, but satisfies wavefunction continuity at the boundary.

Table 1 shows that at higher potential, for example,  $U = 10$  eV, the wave number  $\zeta_{01} = 2.39 \times 10^8$  already approaches the wave number for the infinite quantum well  $\zeta_{01}^{inf} = 2.40 \times 10^8$ , where zero wavefunction is assumed outside the well:

$$J_0(\zeta_{01}^{inf} R) = 0. \tag{20}$$

Therefore, the wavefunctions  $\mu_A(\phi, \rho)$  and  $\mu_B(\phi, \rho)$  inside the quantum well of relatively high potential  $U = 10$  eV are nearly the same as the wavefunctions in the infinite quantum well, as shown in Figure 3. However, contrary to conventional assumptions, the wavefunctions outside the quantum well are not exactly zero; they are reduced but remain nonzero, particularly near the boundary for  $\mu_B(\phi, \rho)$ . This nonzero presence near the boundary significantly contributes to the current density, as will be discussed in the next section. The wavefunctions remain substantial within a narrow region near the boundary, known as the skin depth, but they decay rapidly beyond this region. The skin depth

becomes narrower as the potential increases, similar to the behavior of an optical field confined within a waveguide [14].



**Figure 3.** Wavefunction plot for the Dirac electron in a quantum well of  $U = 10$  eV and  $R = 10$  nm. The large component  $\mu_A(\phi, \rho)$  (left) and small component  $\mu_B(\phi, \rho)$  (right) wavefunctions (blue) inside the quantum well are nearly identical to the wavefunctions (orange) inside an infinite quantum well. The wavefunctions outside the quantum well are diminished but not exactly zero, especially at the boundary for  $\mu_B(\phi, \rho)$ , so that the wavefunction continuity is always satisfied.

#### 4. Evanescent Electron Wave-Spin

We now investigate the spin nature of the evanescent electron wave that resides within the skin depth region outside the quantum well. Analytical expression of the current density is obtained by using the wavefunctions in Equation (17),

$$\begin{aligned}
 j_\rho &= -ec\psi^\dagger \alpha_\rho \psi = 0, \text{ everywhere;} \\
 j_\phi &= -ec\psi^\dagger \alpha_\phi \psi = \begin{cases} -\frac{e\hbar c^2}{\varepsilon + mc^2} \zeta J_0(\zeta\rho) J_1(\zeta\rho), & \rho \leq R \\ -\kappa^2 \frac{e\hbar c^2}{\varepsilon - U + mc^2} \zeta K_0(\zeta\rho) K_1(\zeta\rho), & \rho > R, \end{cases} \quad (21)
 \end{aligned}$$

where  $-e = -1.602 \times 10^{-19}$  C to represent the electron charge.

Equation (21) demonstrates that stable circulating current density exists both inside and outside the quantum well, as evidenced by the non-zero component  $j_\phi$  in all regions and zero component  $j_\rho$  everywhere. The evanescent electron wave is shown to spin concurrently with the electron wave inside the quantum well, as illustrated by the vector plot of Figure 4. The current density continuity is observed at the boundary as a result of the wavefunction continuity at the boundary in Equations (15) and (17), which also ensures the charge density continuity.

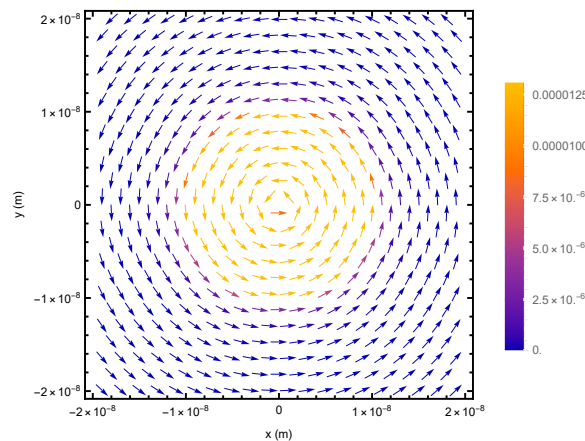


**Figure 4.** Vector plot of the current density for a spin-up ground state electron in a quantum well of  $U = 0.01$  eV and  $R = 10$  nm. The evanescent wave spins concurrently with the wave inside the quantum well.

The analysis highlights that spin is a wave property that persists throughout the entire electron wave.

### 5. Evanescent Electron Wave-Spin Sensing

The discussion above raises questions about the security of spin quantum information and the possibility of novel evanescent electron wave-spin sensing, which is analogous to evanescent optical wave sensing [13–15] that has already been employed in real applications. The evanescent optical wave is part of an eigen electromagnetic wave outside an optic waveguide or fiber that can interact with matters around the waveguide. The main optic wave confined inside the waveguide is perturbed but is largely maintained. Similarly, the evanescent electron wave is a part of an eigen electron wave outside a quantum well that can interact with an electromagnetic wave around the quantum well. The optic and electronic evanescent wave detections share the same fundamental matter–field interaction:  $\mathbf{j}(\mathbf{r}) \cdot \mathbf{A}(\mathbf{r})$ . The interaction is usually small due to the nature of evanescent waves; therefore, the main wave inside the confinement is only perturbed but is not destroyed. Thus, evanescent wave sensing offers a unique detection scheme by enabling partial wave interactions without destroying the main wave inside the confinement, providing a different perspective on the quantum measurement problem [17].

However, the evanescent electron wave contains the spin property as described by the current density  $\mathbf{j}(r)$  in Equation (21). When it interacts with the electromagnetic field  $\mathbf{A}(r)$ , only partial spin participates in the process that could result in the fractional spin effects as discussed in the previous study [9]. Such a partial spin concept conflicts with the particle spin picture, where a single particle electron possesses a unit spin and can only manifest the full spin effect during interaction. In the particle electron spin picture, the electron carrying the full spin tunnels out of the quantum well with a probability density given by the square of the wavefunction  $\psi^\dagger \psi$ . If the spin is detected outside the quantum well, the spin information inside is destroyed since the electron that carries the full spin no longer exists within the quantum well.

The conflicting pictures are illustrated in Figure 5, which comprises two figures for the electron in the same quantum well of  $R = 10$  nm and  $U = 0.01$  eV.

The lower figure illustrates the conventional wave–particle duality picture of the electron by displaying the spinning electron and its probability density. In this framework, the electron carrying the entire spin property can tunnel out of the quantum well with a certain probability. If a measurement detects the spin outside the quantum well, it implies that no electron, hence spin information, remains inside the well.

In contrast, the upper figure depicts the wave-spin interpretation, showing the spinning current density across all regions. In this view, the entire electron wave spins with no probability interpretation. Here, partial spin can be detected without destroying the wave-spin inside the well.

These conflicting views arise from different interpretations of the quantum mechanical wave, and these differences can be tested experimentally. In the conventional quantum mechanics framework, the microscopic world is fundamentally understood through the probabilistic wave–particle duality, where the wave is a statistical abstraction representing the probability distribution of the particle. In contrast, our interpretation posits that the electron is fully described by its wave properties, with the wave itself being the true and sole entity of the electron. Since the wavefunction is a vector in the Hilbert space, the wave properties such as charge density  $e\psi^\dagger \psi$  and current density  $ec\psi^\dagger \alpha \psi$  are deterministic observables. Thus, the electron, in our view, is a concrete, deterministic entity fully characterized by Lorentz-invariant charge and current densities.

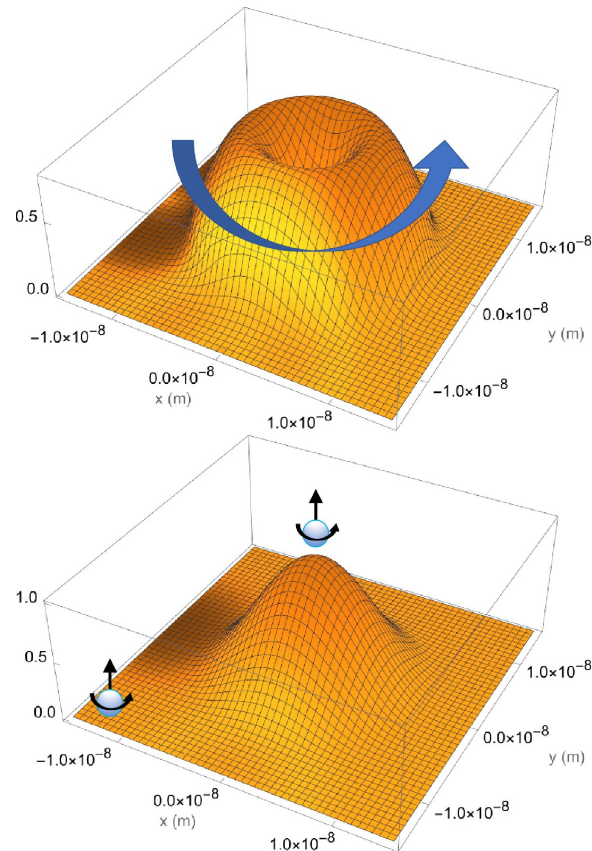


**Figure 5.** Conflicting views on the electron wave and spin in a quantum well of  $R = 10$  nm and  $U = 0.01$  eV. The upper figure presents the wave-spin perspective, illustrating the spinning current density across all regions of the well. In this view, the electron wave exhibits continuous spin, independent of a probability interpretation, allowing partial spin detection without collapsing the wave function within the well. The lower figure depicts the conventional wave-particle duality, showing the electron with its associated spin and probability density. In this framework, the entire spin can tunnel out of the quantum well, and a successful measurement of spin outside the well implies no remaining spin information within the well.

## 6. Discussion

In this work, we have demonstrated the existence of an evanescent electron wave outside both finite and infinite quantum wells. This result was obtained by solving the exact solutions of the Dirac equation for a cylindrical quantum well and applying the continuity conditions of the spinor wavefunction at the boundary. Additionally, we derived analytical expressions for the current density, which show that the evanescent wave exhibits a concurrent spin with the electron wave inside the quantum well.

The existence of a nonzero wavefunction outside an infinite quantum well implies that the electron wave cannot be strictly confined to a mathematical point. Additionally, the vortex topology demonstrated by the electron wave-spin must also be preserved. These observations indicate that the singularities in mass density, and the consequent disruption of geodesics encountered in gravitational and cosmological contexts, may not accurately represent physical reality when the continuity of the Dirac wavefunction and the topological properties of wave-spin are taken into account.

Moreover, the spin of the evanescent wave indicates that quantum information, or quantum entropy, is not entirely confined within the quantum well but can, in fact, extend beyond it. This insight opens up the possibility of accessing or detecting quantum spin information through the evanescent wave without causing a collapse of the entire spin state.

Our results underscore that the electron wave is a real, tangible entity with deterministic properties. This suggests that quantum processes or devices based on the manipulation and probing of electron waves are fundamentally deterministic, rather than probabilistic.

**Author Contributions:** Conceptualization, J.G. and F.S.; investigation, J.G. and F.S.; writing, J.G.; writing—review and editing, F.S.; visualization, J.G. and F.S. All authors have read and agreed to the published version of the manuscript.

**Funding:** This research received no external funding.

**Institutional Review Board Statement:** Not applicable.

**Data Availability Statement:** The original data presented in the study are openly available in arxiv at <https://arxiv.org/abs/2309.17325>, accessed on 29 June 2024.

**Acknowledgments:** The authors wish to acknowledge the helpful discussions with the reviewers of this journal, as well as all the reviewers on the Qeios platform. Their insightful and constructive feedback significantly contributed to the improvement of this work.

**Conflicts of Interest:** The authors declare no conflicts of interest.

## References

1. National Academies of Sciences, Engineering, and Medicine; Sciences, D.; Board, I.; Board, C.; Computing, C.; Horowitz, M.; Grumbling, E. *Quantum Computing: Progress and Prospects*; National Academies Press: Washington, DC, USA, 2019.
2. Kloeffel, C.; Loss, D. Prospects for Spin-Based Quantum Computing in Quantum Dots. *Annu. Rev. Condens. Matter Phys.* **2013**, *4*, 51–81. [[CrossRef](#)]
3. Hirohata, A.; Yamada, K.; Nakatani, Y.; Prejbeanu, I.L.; Diény, B.; Pirro, P.; Hillebrands, B. Review on spintronics: Principles and device applications. *J. Magn. Magn. Mater.* **2020**, *509*, 166711. [[CrossRef](#)]
4. Gerlach, W.; Stern, O. Das magnetische Moment des Silberatoms. *Z. Fur Phys.* **1922**, *9*, 349. [[CrossRef](#)]
5. Uhlenbeck, G.; Goudsmit, S. Spinning Electrons and the Structure of Spectra. *Nature* **1926**, *117*, 264. [[CrossRef](#)]
6. Belinfante, F.J. On the spin angular momentum of mesons. *Physica* **1939**, *6*, 887–898. [[CrossRef](#)]
7. Ohanian, H.C. What is spin. *Am. J. Phys.* **1986**, *54*, 6. [[CrossRef](#)]
8. Gao, J. Electron wave spin in a quantum well. *J. Phys. Commun.* **2022**, *6*, 081001. [[CrossRef](#)]
9. Gao, J.; Shen, F. Electron Spin Topology in Excited States and Fractional Spin Effect. *Qeios* **2023**, *10*, 32388. [[CrossRef](#)]
10. Lima, F.M.S.; Nunes, O.A.C.; Fonseca, A.L.A.; Amato, M.A.; da Silva, E.F. Effect of a terahertz laser field on the electron-DOS in a GaAs/AlGaAs cylindrical quantum wire: Finite well model. *Semicond. Sci. Technol.* **2008**, *23*, 125038. [[CrossRef](#)]
11. Qasem, M.R.; Ben-Ali, Y.; Falyouni, F.; Bria, D. Electron Transport in AlGaAs Cylindrical Quantum Wire Sandwiched between Two GaAs Cylindrical Quantum Well Wires. *Solid State Phenom.* **2022**, *335*, 23–30. [[CrossRef](#)]
12. Bransden, B.H.; Joachain, C.J. *Quantum Mechanics*, 2nd ed.; Pearson Education: Essex, UK, 2000.
13. Huertas, C.S.; Calvo-Lozano, O.; Mitchell, A.; Lechuga, L.M. Advanced evanescent-wave optical biosensors for the detection of nucleic acids: An analytic perspective. *Front. Chem.* **2019**, *7*, 724. [[CrossRef](#)] [[PubMed](#)]
14. Islam, S.; Halder, B.; Refaie Ali, A. Optical and rogue type soliton solutions of the (2+1) dimensional nonlinear Heisenberg ferromagnetic spin chains equation. *Sci. Rep.* **2023**, *13*, 9906. [[CrossRef](#)] [[PubMed](#)]
15. Refaie Ali, A.; Eldabe, N.; El Naby, A. EM wave propagation within plasma-filled rectangular waveguide using fractional space and LFD. *Eur. Phys. J. Spec. Top.* **2023**, *232*, 2531–2537. 023-00934-1 [[CrossRef](#)]
16. Xiao, Z. Spectra of Lorentz-violating Dirac bound states in a cylindrical well. *Phys. Rev. D* **2016**, *94*, 115020. [[CrossRef](#)]
17. Leggett, A.J. The Quantum Measurement Problem. *Science* **2005**, *307*, 871–872. [[CrossRef](#)] [[PubMed](#)]

**Disclaimer/Publisher’s Note:** The statements, opinions and data contained in all publications are solely those of the individual author(s) and contributor(s) and not of MDPI and/or the editor(s). MDPI and/or the editor(s) disclaim responsibility for any injury to people or property resulting from any ideas, methods, instructions or products referred to in the content.